Original Article

Inhalation & intravenous: umbilical cord mesenchymal stem cell-derived exosomes therapy strategy for acute respiratory distress syndrome in a murine model

Luyu Yang[1,2#], Zhimin Cao[3#], Yuanfang Xing[2], Yuanming Pan[2,4], Can Yang[5], Li Zhang[6], Hong Zhao[6*], Teng Ma[2,4*], Huan Ye[1,2*]

[1]Department of Respiratory and Critical Care Medicine, Beijing Chest Hospital, Capital Medical University, Beijing, China; [2]Beijing Tuberculosis and Thoracic Tumor Research Institute, Beijing, China; [3]Department of Respiratory and Critical Care Medicine, Guizhou Provincial People's Hospital, Guiyang, China; [4]Cancer Research Center, Beijing Chest Hospital, Capital Medical University, Beijing, China; [5]Department of Critical Care Medicine, Chengdu Fifth People's Hospital, Chengdu, China; [6]Department of Pathology, Beijing Chest Hospital, Capital Medical University, Beijing, China

Contributions: (I) Conception and design: L Yang, Z Cao; (II) Administrative support: H Ye, T Ma, H Zhao; (III) Provision of study materials or patients: Y Xing, Y Pan; (IV) Collection and assembly of data: C Yang, L Zhang; (V) Data analysis and interpretation: L Yang, Z Cao; (VI) Manuscript writing: All authors; (VII) Final approval of manuscript: All authors.

[#]These authors contributed equally to this work as co-first authors.

[*]These authors contributed equally to this work.

Correspondence to: Professor Huan Ye, MD. Department of Respiratory and Critical Care Medicine, Beijing Chest Hospital, Capital Medical University, Beijing, China; Beijing Tuberculosis and Thoracic Tumor Research Institute, Courtyard 1, No. 9 Beiguan Street, Tongzhou District, Beijing 101199, China. Email: yedahuan@yeah.net.

Background: Acute respiratory distress syndrome (ARDS) is a complex syndrome characterized by acute diffuse lung injury and progressive respiratory failure, caused by various intra- and extra-pulmonary factors. The coronavirus disease 2019 (COVID-19) pandemic has significantly increased the incidence of ARDS, posing a tremendous threat to human health due to its high mortality rate and lack of effective therapeutic drugs. In recent years, mesenchymal stem cell-derived exosomes (MSC-exo) have been considered a new hope for the treatment of ARDS due to their potent immunomodulatory characteristics. Although multiple studies have demonstrated their efficacy and safety, the differential therapeutic effects of various administration routes and doses remain unclear. This study aimed to investigate the administration route of MSC-exo for ARDS treatment, with the goal of maximizing therapeutic benefits and providing valuable clinical insights.

Methods: This study aims to establish an ARDS disease model by intratracheal instillation of lipopolysaccharide (LPS) in male C57/BL6 mice. Subsequently, umbilical cord mesenchymal stem cell exosomes will be administered via three methods: inhalation, tail vein injection, and combination therapy (inhalation combined with tail vein injection). Following the establishment of the mouse ARDS model via intratracheal instillation of LPS, the animals were randomly divided into seven groups based on the timing and dosage of the treatment administration. Samples were harvested at 24 hours, 72 hours, and 7 days after modeling. The assessments included RNA transcriptome sequencing, cytokine levels in blood and bronchoalveolar lavage fluid, blood oxygen saturation, histopathological staining, and survival analysis.

Results: Compared to nebulized exosomes alone, dual-route administration significantly improved respiratory function, as evidenced by prolonged expiratory and inspiratory times and increased minute ventilation ($P \leq 0.05$). Furthermore, it decreased the levels of the pro-inflammatory cytokines interleukin-1β (IL-1β) and interleukin-6 (IL-6) in the blood ($P=0.01$, $P=0.041$). Compared to intravenous exosomes alone, dual-route administration produced broader improvements. It significantly enhanced lung function by prolonging expiratory time ($P=0.01$), inspiratory time ($P=0.004$), and increasing minute ventilation ($P=0.02$). Additionally, it suppressed inflammation by lowering IL-6 levels in bronchoalveolar lavage fluid ($P=0.01$) and reduced the death of type II alveolar epithelial cells ($P=0.03$).

Conclusions: The dual-route administration of umbilical cord MSC-exo is more effective in controlling the inflammatory response and alleviating lung injury in LPS-induced ARDS animal models. Inhalation rapidly alleviates pulmonary inflammation with a smaller dose, while intravenous injection better manages the systemic inflammation. This dual-route approach holds promise as a novel ARDS treatment strategy.

Keywords: Acute respiratory distress syndrome (ARDS); acute lung injury; mesenchymal stem cell-derived exosomes; inhalation; tail vein injection

Submitted Feb 07, 2025. Accepted for publication Sep 29, 2025. Published online Dec 29, 2025.
doi: 10.21037/jtd-2025-250
View this article at: https://dx.doi.org/10.21037/jtd-2025-250

Introduction

Acute respiratory distress syndrome (ARDS) is an acute respiratory disease characterized by severe hypoxemia resulting from non-cardiogenic pulmonary edema and diffuse pulmonary infiltration, as observed by chest imaging (1). ARDS exhibits severe clinical symptoms and a high mortality rate, ranging from 43% to 73% (2). Since the onset of the coronavirus disease 2019 (COVID-19) pandemic, ARDS has become a leading cause of death in COVID-19 patients, with approximately 81% of severe COVID-19 cases progressing to ARDS, posing a grave threat to human life and health (3). During the development of ARDS, inflammatory cells accumulate in the lungs and release a large number of pro-inflammatory cytokines, causing damage to vascular endothelial and alveolar epithelial cells (4). This leads to increased epithelial permeability and eventual disruption of the pulmonary microvascular barrier and the blood-gas barrier, which are key aspects of ARDS pathogenesis (5).

Various treatment methods for ARDS exist in clinical practice, including protective lung ventilation, fluid management, extracorporeal membrane oxygenation (ECMO), and symptomatic supportive treatment (6). However, each of these methods has its pros and cons. For instance, protective lung ventilation may lead to mechanical ventilation-related adverse events, such as difficulty in weaning. Research has indicated that fluid restrictive management can improve oxygenation in patients but does not decrease long-term mortality (7). ECMO, while effective, is associated with high costs, technical challenges, and catheter-related infections. Therefore, there remains an urgent need to explore effective ARDS treatments.

Exosomes are extracellular vesicles measuring approximately 30–120 nm in diameter and containing a variety of bioactive factors, including growth factors, cytokines, and microRNAs (miRNAs), similar to their source cells. Compared to traditional stem cell therapy, mesenchymal stem cell-derived exosomes (MSC-exo) offer advantages in terms of safety and immunogenicity (8,9). Numerous studies have demonstrated the potential

Highlight box

Key findings

- The dual-route administration of umbilical cord mesenchymal stem cell-derived exosomes (MSC-exo) is more effective in controlling the inflammatory response and alleviating lung injury in lipopolysaccharide-induced acute respiratory distress syndrome (ARDS) animal models. Inhalation rapidly alleviates pulmonary inflammation with a smaller dose, while intravenous injection better manages the systemic inflammation.

What is known and what is new?

- Currently, multiple studies have demonstrated that exosomes can treat various lung diseases, including ARDS. Intravenous injection of MSC-exo is one of the important administration routes for cell-free therapy, but it still shows limited efficacy in some patients. As an emerging administration method in recent years, nebulized inhalation therapy can deliver exosomes directly to the lungs, improving lung injury and alleviating patient symptoms. However, studies have found that nebulized administration also presents issues such as airway reactivity and varying therapeutic outcomes due to differences in dosage.
- This study proposes, for the first time, a novel approach of combination therapy, adopting tailored treatment measures for different patients.

What is the implication, and what should change now?

- We propose a novel clinical administration strategy for MSC-exo in treating ARDS, featuring personalized treatment regimens for different patients. This approach paves the way for a new model of cell-free therapy for ARDS. In the future, we will delve into the underlying mechanisms and complement the current ongoing preclinical and clinical studies. These efforts will contribute significantly to the advancement of ARDS treatment.

of exosomes in treating various lung diseases, including ARDS, lung cancer, and pulmonary fibrosis (10-12). MSC-exo is emerging as a cell-free alternative for ARDS therapy (13). Intravenous injection of MSC-exo has shown promise as a critical administration route in clinical studies, although its efficacy varies among patients (14). Nebulized inhalation therapy, a recent administration route, enables targeted delivery of exosomes to the lungs, improving lung injury, and alleviating symptoms (15). However, nebulized administration presents challenges related to varying doses, including airway reactivity and differences in efficacy.

Based on the existing literature, we found that the lipopolysaccharide (LPS) induced ARDS animal disease model can simulate the basic characteristics of human ARDS, including endothelial cell damage and inflammatory status (16). Therefore, we hypothesize that for the LPS-induced ARDS mouse model, MSC-exo administration via intravenous injection can effectively control systemic inflammation, while nebulized inhalation of MSC-exo can address local lung inflammation and injury, resulting in enhanced therapeutic effects. To test this hypothesis, we induced the ARDS model in C57/BL6 mice using LPS intratracheal instillation. We administered exosomes from umbilical cord mesenchymal stem cells through nebulized inhalation, tail vein injection, and dual-route administration, comparing their therapeutic effects with single nebulization or single intravenous administration. This study was designed to develop a novel and more efficient personalized exosome administration strategy for the clinical treatment of ARDS. We present this article in accordance with the ARRIVE reporting checklist (available at https://jtd.amegroups.com/article/view/10.21037/jtd-2025-250/rc).

Methods

Animals and experimental design

A protocol was prepared before the study without registration. The experiments were performed under a project license (No. xk2022-080) granted by the Animal Experiment Ethics Committee of Beijing Chest Hospital, Capital Medical University, in compliance with the institutional guidelines for the care and use of animals. Male C57/BL6 mice aged 6–8 weeks were obtained from Beijing Vital River Laboratory Animal Technology Co., Ltd. (Beijing, China). They were housed at the animal facility of Beijing Chest Hospital, Capital Medical University. Mice were kept in specific pathogen-free (SPF) environments with sterilized food and water, maintaining a room temperature of 25–26 ℃, and alternating light and dark cycles of 10 and 14 hours, respectively. Animals are excluded from the study if any of the following conditions are observed: severe dehydration, lack of exercise, skin damage, persistent tremors, or respiratory failure. Before the experiment, all parameters such as body weight, status and lung function were tested to ensure baseline consistency.

The sample size for this study was determined based on previously published studies in the relevant field, which typically used 5–6 mice per group. However, as multiple key indicators required sampling from different animals and could not be obtained from a single subject, we increased the sample size to 16 mice per group. To account for potential attrition during the experimental process, the final sample size was set at approximately 17 animals per group. This approach ensures the comparability of our study and provides sufficient statistical power for detection (15). No adverse time was observed during the experiment and no data or samples were lost. Throughout the entire experiment, only the author was aware of the grouping situation. A total of 120 male C57/BL6 mice aged 6–8 weeks were induced with ARDS model using intratracheal instillation of LPS (50 μL/30 g, 15 mg/mL, 055:B5). We adopted a completely randomized design approach, numbering the animals one by one, and then using a random number table to group the animals into No-LPS, normal dose exosomes nebulization (Exo-Inh, 0.002×10^9 vesicles per animal), normal-dose exosome tail vein injection (Exo-iv, 1.000×10^9 vesicles per animal), and exosome dual-route administration (Exo-co, 1.002×10^9 vesicles per animal), with both nebulization and tail vein injection. To address differences in dosage between single nebulization and single tail vein injection, we also included high-dose exosome nebulization (Exo-Inh-H, 1.002×10^9 vesicles per animal) and high-dose exosome tail vein injection (Exo-iv-H, 1.002×10^9 vesicles per animal) groups based on the above three different routes of administration. We also added the phosphate-buffered saline (PBS) group. This group misted the mice with PBS after modeling to determine the therapeutic effect of exosomes. Exosome treatment was administered 3 hours post-LPS instillation, while the control group received PBS treatment (17). We evaluated changes in oxygen saturation, lung function, lung tissue damage, and inflammatory factor levels at three time points after treatment: 24 hours, 72 hours, and 7 days post-administration (10) (*Figure 1*). When collecting samples, multiple people work simultaneously to ensure

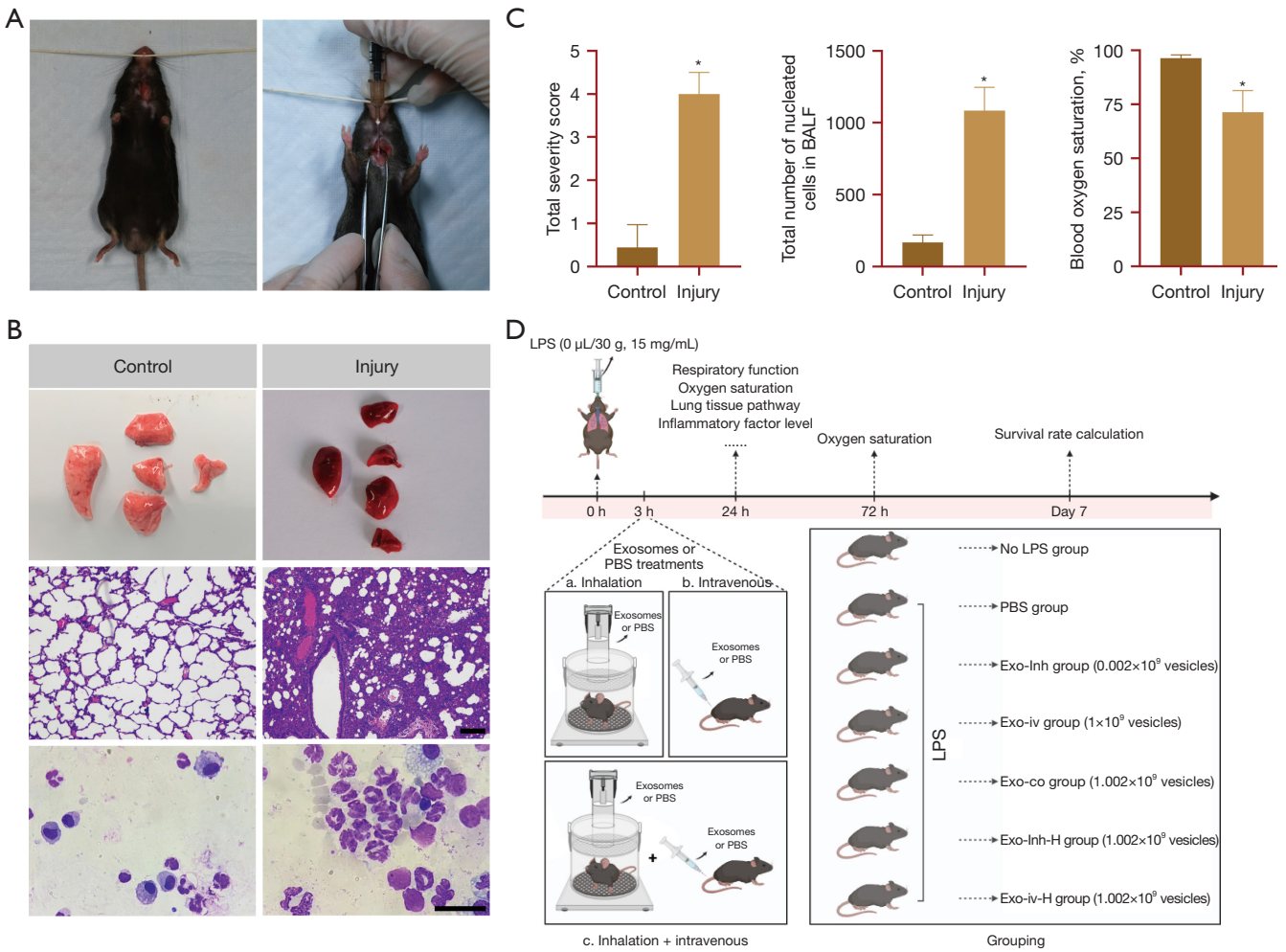

Figure 1 Construction of an ARDS animal model. (A) LPS was administered through airway incision to induce ARDS in mice. (B) Macroscopic view of lung lobes 24 hours after LPS administration. Wright's staining. Scale bar: top, 50 μm; bottom, 100 μm. (C) Evaluating the model, including: total severity score, total number of nucleated cells in BALF, blood oxygen saturation. (D) Research schematic diagram. *, P<0.05 *vs.* control. ARDS, acute respiratory distress syndrome; BALF, bronchoalveolar lavage fluid; Exo-co, exosome dual-route administration; Exo-Inh, exosome nebulization; Exo-Inh-H, high-dose exosome nebulization; Exo-iv, exosome tail vein injection; Exo-iv-H, high-dose exosome tail vein injection; LPS, lipopolysaccharide; MSC-exo, mesenchymal stem cell-derived exosomes; PBS, phosphate-buffered saline.

the accuracy and consistency of the collection time points, thereby reducing errors. During this process, the personnel responsible for sampling and measurement were blinded to the group assignment.

We tested different ink doses (50, 75, 100 μL) to determine the best concentration for even lung distribution. After euthanizing the mice and removing their lungs, we assessed the ink's coverage area. Intratracheal administration of LPS was performed under isoflurane (Youcheng, Hong Kong, China) sedation. To verify the successful establishment of the model, changes in mouse behavior (not shown), fur color (not shown), secretions (not shown), oxygen saturation, lung function, lung tissue damage, and neutrophils in bronchoalveolar lavage fluid (BALF) were observed after administration (*Figure 1*).

Collection of mouse BALF

Mice were euthanized via cervical dislocation following anesthesia, and BALF was collected by injecting 0.6 mL of

PBS into the trachea with a 1 mL syringe, gently aspirating 3 times, collecting the recovered fluid and centrifuging (3,000 rpm, 10 min). The supernatant after centrifugation was saved for cell factor measurement. The precipitated cells were resuspended and counted and classified for nucleated cells.

Characterization of exosome features

Exosomes were obtained from Shandong Qilu Cells Co., Ltd. (Jinan, China) and were cultured in Dulbecco's modified Eagle's medium (DMEM; Gibco, USA), which was supplemented with 10% exosome-depleted fetal bovine serum (Gibco) and 1% penicillin/streptomycin (Gibco), at cellular incubation conditions (37 ℃ and 5% CO_2). Prior to use, the size of all exosome samples was analyzed using nanoparticle tracking analysis (NTA) technology (NanoSight, Malvern, Malvern, UK), and their morphology was analyzed by transmission electron microscopy (TEM). Additionally, they were further confirmed by immunoblotting with known exosome markers CD63 (Ab68418, Abcam, Cambridge, UK), TSG101 (Ab125011, Abcam), CD9 (20597-1-AP, Proteintech, Cambridge, UK) and GM130 (11308-1-AP, Proteintech).

TEM

Exosomes were fixed in 20% paraformaldehyde, loaded onto 200 mesh carbon-coated grids, dried with a Gatan CP3 automatic plunger (Gatan, Inc., Pleasanton, USA), and immersed in liquid ethane, stored in liquid nitrogen until use. Frozen specimens were transferred to a Gatan 914 cryo-holder and maintained at a temperature below −176 ℃ within the microscope. Samples were inspected with a TECNAI G2 microscope (FEI Company, now part of Thermo Fisher Scientific, Waltham, USA) operating at an accelerating voltage of 120 kV. Images were taken with a digital micrograph (Gatan).

Mouse function assessment

Conscious mice were placed in a whole-body plethysmograph (WBP) system (Shanghai Tower Intelligent Technology Co., Ltd., Shanghai, China). After allowing the animals to acclimate, we measured lung function indicators, including inspiratory time (IT), expiratory time (ET), tidal volume (TV), minute ventilation (MV), respiratory rate (RR). Arterial blood was taken from the mouse abdominal aorta and mouse oxygen saturation was measured using a handheld blood analyzer (Abbott, Shanghai, China).

Tissue histopathological staining

Fresh lung tissue was collected, fixed, dehydrated, and embedded in paraffin. We performed hematoxylin and eosin staining on paraffin-embedded tissue sections. The paraffin blocks were cut into 4-μm thick slices, placed on slides, and stained with hematoxylin and eosin (H&E). Images were captured with a Nikon microscope (Nikon E200, Tokyo, Japan). Quantitative analysis of tissue damage was conducted using the "Lung Injury Scoring System" specified by the American Thoracic Society. The results were analyzed by a pathologist who had no prior knowledge of the experimental design and handling.

Tissue immunofluorescence

Fresh lung tissue was collected, fixed, dehydrated, and embedded in optimal cutting temperature compound for quick freezing. Immunofluorescence and *in-situ* cell apoptosis detection were performed on fast-frozen tissue, with slices cut into 15-μm thickness. Tissue sections were permeabilized with 0.3% triton solution and blocked with 3% donkey serum. Immunofluorescence experiments used AQP5 (ab78486, Abcam), SFTPC (ab90716, Abcam), CD31 (AF3628, R&D, Minneapolis, USA) antibodies, at a 1:150 dilution ratio. Terminal deoxynucleotidyl transferase dUTP Nick End Labeling (TUNEL) staining was performed using an *in-situ* cell apoptosis detection kit (C1090, Beyotime, Hunan, China). Images were acquired with a laser confocal microscope (Olympus V1000, Tokyo, Japan).

Enzyme-linked immunosorbent assay (ELISA)

A variety of factors in peripheral blood and BALF were measured using ELISA kits: interleukin (IL)-1β (Raybiotech, Atlanta, USA), IL-6 (Raybiotech), CRP (Byabscience Biotechnology Co., Ltd., Nanjing, China), bicinchoninic acid assay (BCA) (CW2011, Kangwei Century, Jiangsu, China).

RNA-sequencing (RNA-seq) analysis

Sample quality control RNA integrity was assessed using the RNA Nano 6000 Assay Kit of the Bioanalyzer 2100 system (Agilent Technologies, CA, USA). Specifically, the

lungs were collected from ARDS group and Exo-co group. Differential expression analysis was performed on samples with biological replicates using DESeq2 software (1.20.0) for differential expression analysis between two comparison combinations.

Statistical analysis

Statistical analysis was conducted using GraphPad Prism 7 software (GraphPad Software, San Diego, CA, USA). All results are presented as mean ± standard deviation (SD). Paired Student's *t*-test was used for comparisons between two groups. Non-parametric one-way analysis of variance (Kruskal-Wallis test) was used for comparisons among three or more groups. For the Bonferroni *post-hoc* correction for multiple comparisons, the differences in the *post-hoc* comparisons were considered statistically significant if the Bonferroni-adjusted P value (P_adj) was ≤0.05. Please revise and update the statistical results.

Results

Establishment of an ARDS mouse model using LPS intratracheal instillation

Intratracheal instillation of LPS is a common method for inducing lung injury in mice and establishing ARDS animal models (16). In this study, we successfully induced the ARDS model in C57/BL6 mice by intratracheally instilling a single high dose of LPS (*Figure 1A*). Throughout the study, we monitored the mice's body weight as an indicator of disease progression. According to the official workshop of the American Thoracic Society, key features of experimental ARDS in animals include rapid onset (within 24 hours), histological evidence of lung injury, alterations in the alveolar capillary barrier, an inflammatory response, and physiological dysfunction. Among these, tissue injury is a prominent feature (18). Therefore, we chose to assess lung tissue 24 hours after treatment to confirm the successful establishment of the model. Compared with normal mouse lungs, the lungs of the injured mice displayed severe pulmonary edema and extensive lung tissue congestion. H&E staining of both groups revealed substantial neutrophil infiltration in the alveoli or alveolar septa, accompanied by notable thickening of the alveolar walls (*Figure 1B*). High-magnification Wright's staining of the injured mice's lavage fluid showed a large number of neutrophils (*Figure 1B)*. Furthermore, the injured mice exhibited increased periorbital secretions (not shown), reduced oxygen saturation, increased lung injury scores and increased number of nucleated cells in lavage fluid, all confirming the successful establishment of the ARDS model (*Figure 1C*).

Characteristics of exosomes derived from umbilical cord mesenchymal stem cells

The MSC-exo used in this study were extracted and purified from the supernatant of cultured human umbilical cord mesenchymal stem cells from the 4th to 6th generations. We performed a comprehensive characterization of these MSC-exo, including assessments of their size, morphology, and the presence of common exosome markers. The exosomes were validated by their expression of CD9, and TSG101, while notably lacking GM130, consistent with previous reports (19) (*Figure 2A*). NTA revealed an average particle size of 79.93 nm for MSC-exo (20) (*Figure 2B*). Additionally, electron microscopy revealed the typical cup-shaped or ring-like structure of exosomes, in accordance with previous research (21) (*Figure 2C*).

Dual-route administration of MSC-exo via inhalation and intravenous injection improves respiratory function and survival status in mice

In clinical settings, ARDS typically presents with acute onset, characterized by progressive respiratory failure and refractory hypoxemia. Based on these clinical features, we monitored the respiratory function and oxygen saturation of mice at 24 hours. In addition, for the sake of overall rigor, we also investigated blood oxygen saturation in mice 3 hours after modeling to ensure drug efficacy. We found that except for the Exo-iv and PBS groups, the blood oxygen saturation of mice in other groups did not decrease further after treatment. The results showed that at 24 hours, oxygen saturation in the PBS group of mice was 71%. After MSC-exo treatment, oxygen saturation improved in the Exo-co, Exo-Inh, Exo-Inh-H, Exo-iv, and Exo-iv-H groups, with statistically significant differences observed between the Exo-co group and the Exo-Inh, Exo-Inh-H, and Exo-iv groups, but not the Exo-iv-H group. At 72 hours, the oxygen saturation in the PBS group was 80%, and overall, it improved in the Exo-co, Exo-Inh, Exo-Inh-H, Exo-iv, and Exo-iv-H groups compared to 24 hours (*Figure 3*). We examined the 24-hour respiratory function of the mice, including ET, IT, RR, TV, and MV. The Exo-co group showed prolonged ET and IT and increased MV compared

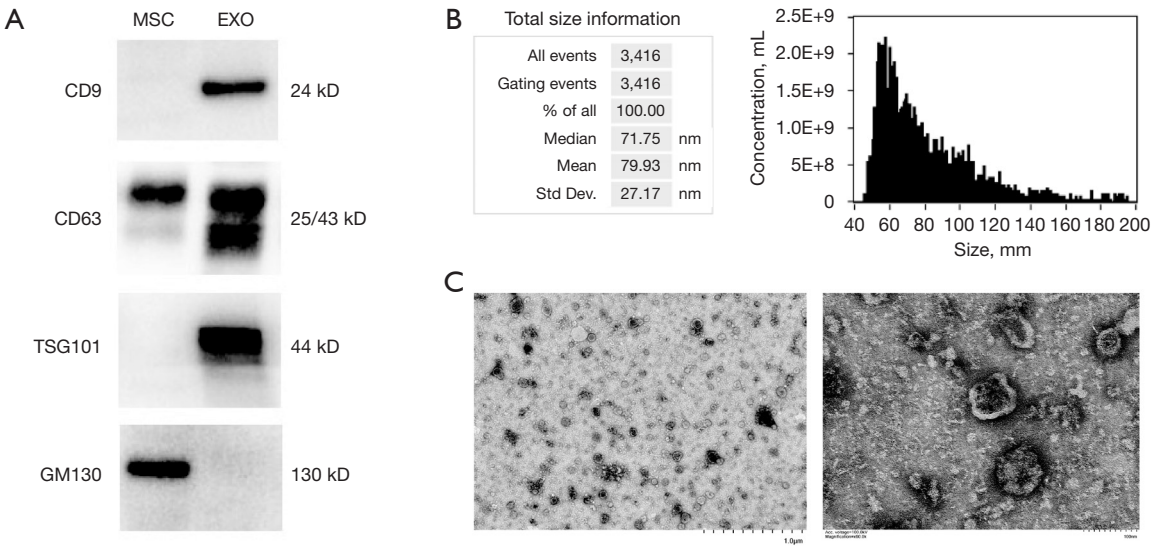

Figure 2 Analysis of MSC-exo. (A) Immunoblot analysis of CD9, CD63, TSG101, and GM130 proteins in MSC-exo. (B) Size analysis of fresh MSC-exo particles using NanoSight. (C) Representative images of MSC-exo captured by transmission electron microscopy. Scale bar: 1.0 μm on the left, 100 nm on the right. MSC-exo, mesenchymal stem cell-derived exosomes.

to the Exo-Inh, Exo-Inh-H, Exo-iv, and Exo-iv-H groups (P_{ET} =0.050, P_{ET} =0.050, P_{ET} =0.005, P_{ET} =0.01; P_{IT} =0.01, P_{IT} =0.02, P_{IT} =0.004, P_{IT} =0.002, respectively). When we used the same administration method but changed the dose, the Exo-Inh group had longer ET and IT and increased MV compared to the Exo-Inh-H group, while there was no significant difference between the Exo-iv and Exo-iv-H groups (*Figure 3A-3F*). In addition, we calculated the 7-day survival rate of the mice; all five mice in the PBS group died on the third day, resulting in a survival rate of 0%, while after MSC-exo treatment, all five mice in the Exo-co group survived, for a survival rate of 100%. The survival rates for the Exo-Inh, Exo-iv, and Exo-iv-H groups were 60%, 80%, and 80%, respectively, whereas the Exo-Inh-H group reached 40% (*Figure 3G*).

Dual-route administration of MSC-exo via inhalation and intravenous injection mitigates lung tissue damage in mice

To further explore the impact of different administration methods on mouse lung histology, we stained paraffin sections of lung tissue from each group with H&E. The results showed that, regardless of the administration method, all groups treated with MSC-exo showed thinner alveolar septa, reduced neutrophil infiltration in the alveoli or alveolar septa, and decreased alveolar cavity exudation compared to the PBS group. However, due to different administration methods, the extent of lung injury reduction varied among groups (*Figure 4A*). Quantification of lung injury, following the criteria of the American Thoracic Society, showed that the Exo-co group had lower lung injury scores compared to the Exo-Inh and Exo-iv groups (18) (P_{Inh} =0.050, P_{iv} =0.01). Eliminating the influence of dosage differences, the Exo-co group still demonstrated greater lung injury reduction and lower lung injury scores relative to the Exo-Inh-H and Exo-iv-H groups. In cases with identical administration methods, investigation into the effect of varying doses revealed that the Exo-Inh group was superior in reducing lung tissue damage, resulting in a lower lung injury score compared to the Exo-Inh-H group (P=0.004), with no significant difference found between the Exo-iv and Exo-iv-H groups (*Figure 4B-4E*).

Pulmonary gas exchange occurs in alveoli, the terminal structures of the distal airway, which are lined by two types of epithelial cells (22). Alveolar epithelium consists of type I alveolar epithelial cells (AT1) and type II alveolar epithelial cells (AT2). The former mediates gas exchange, while the latter produces and releases crucial molecules for lung injury defense responses and homeostasis maintenance, such as pulmonary surfactant and cytokines (23,24). To further validate the impact of different administration methods on the fine structure within the lung, we tested the distribution and quantity changes of AT1 and AT2 in mouse lung tissue from each group. Immunofluorescence

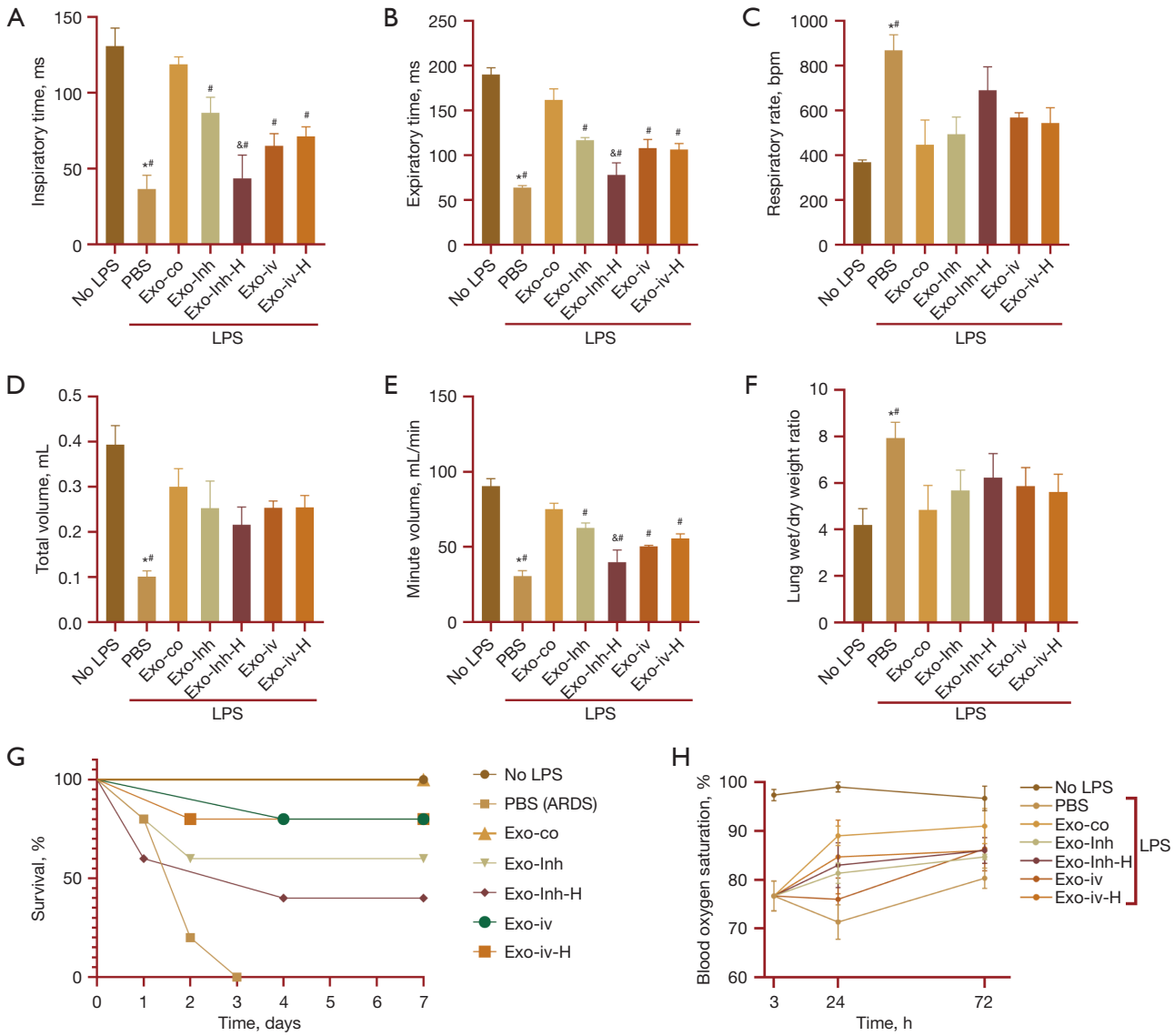

Figure 3 MSC-exo dual channel therapy improves respiratory function and survival rate of ARDS mice. Inspiratory time (A), expiratory time (B), respiratory rate (C), total volume (D), minute volume (E), and lung wet/dry weight ratio (F) 24 hours after LPS intervention in mice, N=6 animals. (G) Survival within 7 days of disease progression. N=5 animals. (H) O_2 saturation at 24 and 72 hours following LPS/vehicle injection. N=3 animals. *, P<0.05 *vs.* no LPS; #, P<0.05 *vs.* Exo-co; &, P<0.05 *vs.* Exo-Inh. ARDS, acute respiratory distress syndrome; Exo-co, exosome dual-route administration; Exo-Inh, exosome nebulization; Exo-Inh-H, high-dose exosome nebulization; Exo-iv, exosome tail vein injection; Exo-iv-H, high-dose exosome tail vein injection; LPS, lipopolysaccharide; MSC-exo, mesenchymal stem cell-derived exosomes; PBS, phosphatebuffered saline.

results of AT1 marked by aquaporin-5 (AQP5) and AT2 marked by surfactant protein C (SFTPC) showed that the quantity of AT1 and AT2 in the lungs of mice from all groups increased after MSC-exo treatment compared to the PBS treatment group, but the extent varied due to different administration methods (*Figure 5*). Consistent with HE staining results, whether for AT1 or AT2, the Exo-Inh group was superior to the Exo-Inh-H group in reducing the loss of alveolar epithelial cells (P_{AT1} =0.048, P_{AT2} ≤0.01); there was no significant difference between the Exo-iv and Exo-iv-H groups. Quantitative results of AQP5 immunostaining showed that under the same dose, the Exo-

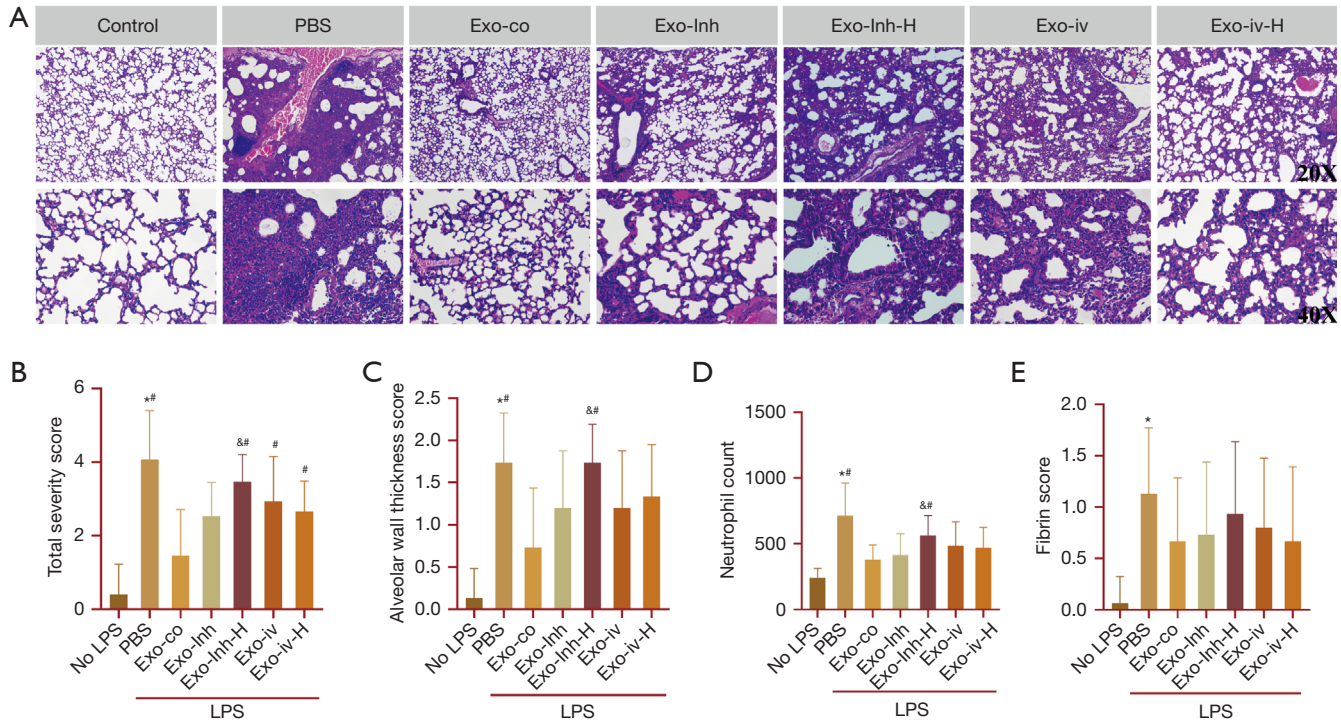

Figure 4 MSC-exo dual channel therapy mitigates lung injury in ARDS animal model. (A) Representative H&E staining. Scale bar: top, 50 μm; bottom, 100 μm. (B-E) Quantification of lung damage according to American Thoracic Society guidelines: total severity score (B), alveolar wall thickness (C), neutrophil count in lung tissue (D), and fibrin accumulation (E). N=5 animals. Scores was averaged from one blinded and two non-blinded scorers. *, P<0.05 *vs.* no LPS; #, P<0.05 *vs.* Exo-co; &, P<0.05 *vs.* Exo-Inh. ARDS, acute respiratory distress syndrome; Exo-co, exosome dual-route administration; Exo-Inh, exosome nebulization; Exo-Inh-H, high-dose exosome nebulization; Exo-iv, exosome tail vein injection; Exo-iv-H, high-dose exosome tail vein injection; H&E, hematoxylin and eosin; LPS, lipopolysaccharide; MSC-exo, mesenchymal stem cell-derived exosomes; PBS, phosphatebuffered saline.

co group could alleviate the physical damage to AT1 caused by LPS compared to the Exo-Inh-H group, but there was no significant difference compared to the Exo-iv-H group (*Figure 6*). Quantitative results of SFTPC immunostaining showed that the number of AT2 cells in the Exo-co group was significantly higher than that in the Exo-iv, Exo-Inh-H, and Exo-iv-H groups, but not the Exo-Inh group (*Figure 6C*).

In ARDS patients, alveolar capillary endothelial damage leads to increased permeability and the occurrence of pulmonary edema (25). CD31, also known as platelet endothelial cell adhesion molecule-1, is a 130-kDa transmembrane protein that is constitutively expressed at endothelial cell-cell junctions. Increasing evidence suggests that CD31 helps maintain vascular integrity and can restore vascular integrity after barrier disruption (26,27). Therefore, we used CD31 to characterize vascular endothelial cells and observe their injury among groups. Immunofluorescence results of CD31 showed that all groups demonstrated the effectiveness of MSC-exo in reducing vascular endothelial cell injury, but there were no significant statistical differences among groups (*Figure 5*, *Figure 6D*). The total protein in BALF, another indicator reflecting changes in vascular permeability, also showed the same results (*Figure 7*).

Usually, there is a significant increase in apoptosis of lung epithelial and endothelial cells in ARDS patients (28). Our research shows that Exo-co group can significantly reduce the number of apoptotic cells in the lungs of diseased mice (*Figure 6A,6E*).

Dual-route administration of MSC-exo via airway nebulization and intravenous injection alleviates global and local pulmonary inflammation in LPS-induced ARDS

To further understand how different administration methods impact systemic and local pulmonary inflammation in ARDS mice, we analyzed the changes in inflammatory

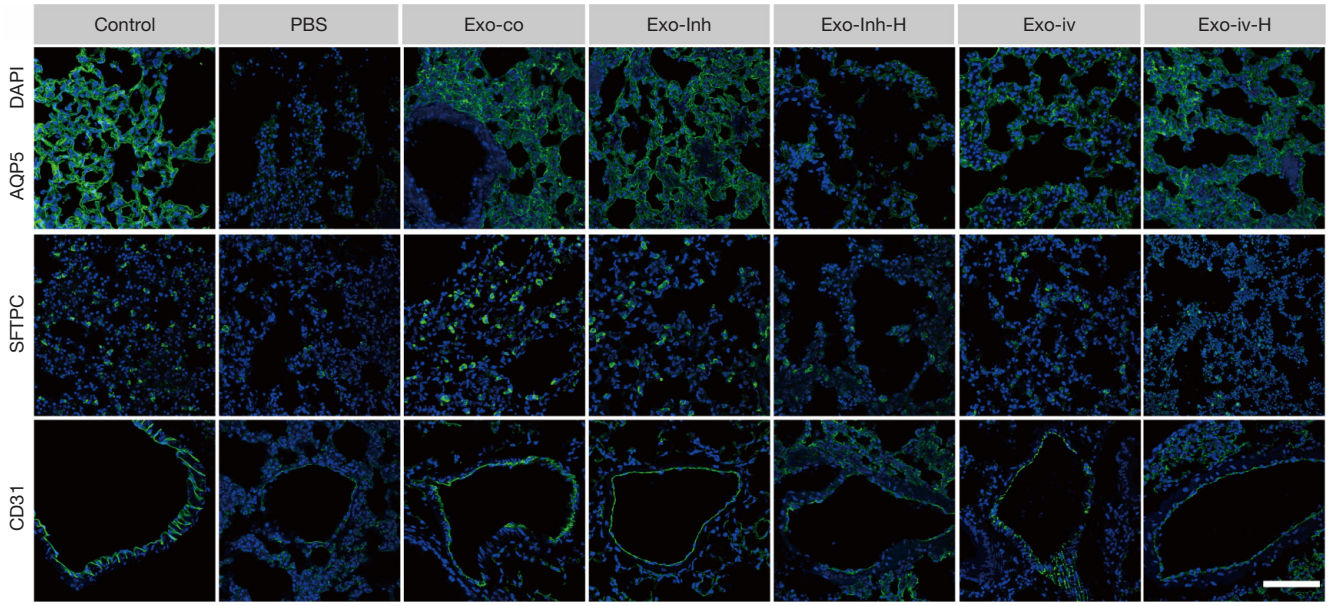

Figure 5 MSC-exo dual channel therapy alleviates damage to alveolar epithelial and vascular endothelial cells. Immunofluorescence staining of lung sections for AQP5 (specifically expressed in AT1 cell), SFTPC (specifically expressed in AT2 cell), and CD31 (generally as a marker protein of vascular endothelial cell). N=5 animals; Scale bar =100 μm. AQP5, aquaporin 5; CD31, platelet endothelial cell adhesion molecule-1; DAPI, 4',6-diamidino-2-phenylindole; Exo-co, exosome dual-route administration; Exo-Inh, exosome nebulization; Exo-Inh-H, high-dose exosome nebulization; Exo-iv, exosome tail vein injection; Exo-iv-H, high-dose exosome tail vein injection; MSC-exo, mesenchymal stem cell-derived exosomes; PBS, phosphatebuffered saline; SFTPC, surfactant protein C.

cytokines in both peripheral blood and BALF. Two pivotal cytokines, IL-6 and IL-1β, known regulators of severe cytokine storms, were examined. Within peripheral blood, comparisons of the same administration method but different concentrations revealed significantly lower levels of IL-6 and IL-1β in the Exo-Inh group compared to the Exo-Inh-H group (P_{IL-6} =0.01, $P_{IL-1β}$ =0.044). There was no significant difference between the Exo-iv and Exo-iv-H groups. Under different administration methods, the Exo-co group could reduce the levels of IL-6 and IL-1β more than the Exo-Inh group (P_{IL-6} ≤0.01, $P_{IL-1β}$ ≤0.01), but there was no significant statistical difference compared to the Exo-iv group. To eliminate the bias caused by dosage differences, we further explored the differences in reducing LPS-induced inflammation under the same dosage with different administration methods. The results showed that compared with the Exo-Inh-H and Exo-iv-H groups, the Exo-co group had a significant statistical difference in reducing the level of IL-1β in peripheral blood (P_{Inh-H} ≤0.01, P_{iv-H} =0.02). Additionally, the Exo-co group had a lower IL-6 level compared to the Exo-Inh-H group (*Figure 7A*,*7B*).

C-reactive protein (CRP), an important acute phase reactant of ARDS, is an important measure of the inflammatory state (29). Therefore, in this study, we measured CRP and found that the Exo-co group could significantly reduce the peripheral blood CRP level in ARDS mice compared to the Exo-Inh-H group, but there was no significant statistical difference compared to the Exo-iv-H group. However, consistent with the above results, the CRP level of the Exo-Inh group was still lower than that of the Exo-Inh-H group (*Figure 7C*).

In BALF, the Exo-Inh group demonstrated lower levels of the aforementioned two cytokines than the Exo-Inh-H group. Moreover, the Exo-co group significantly outperformed the Exo-Inh-H, Exo-iv, and Exo-iv-H groups in reducing IL-6 levels (*Figure 7E*,*7F*). The inflammatory response in ARDS involves both cellular and humoral responses, with the cellular response involving neutrophils, monocytes, and lymphocytes (30). Analyzing the total number of nucleated cells and the proportion of neutrophils

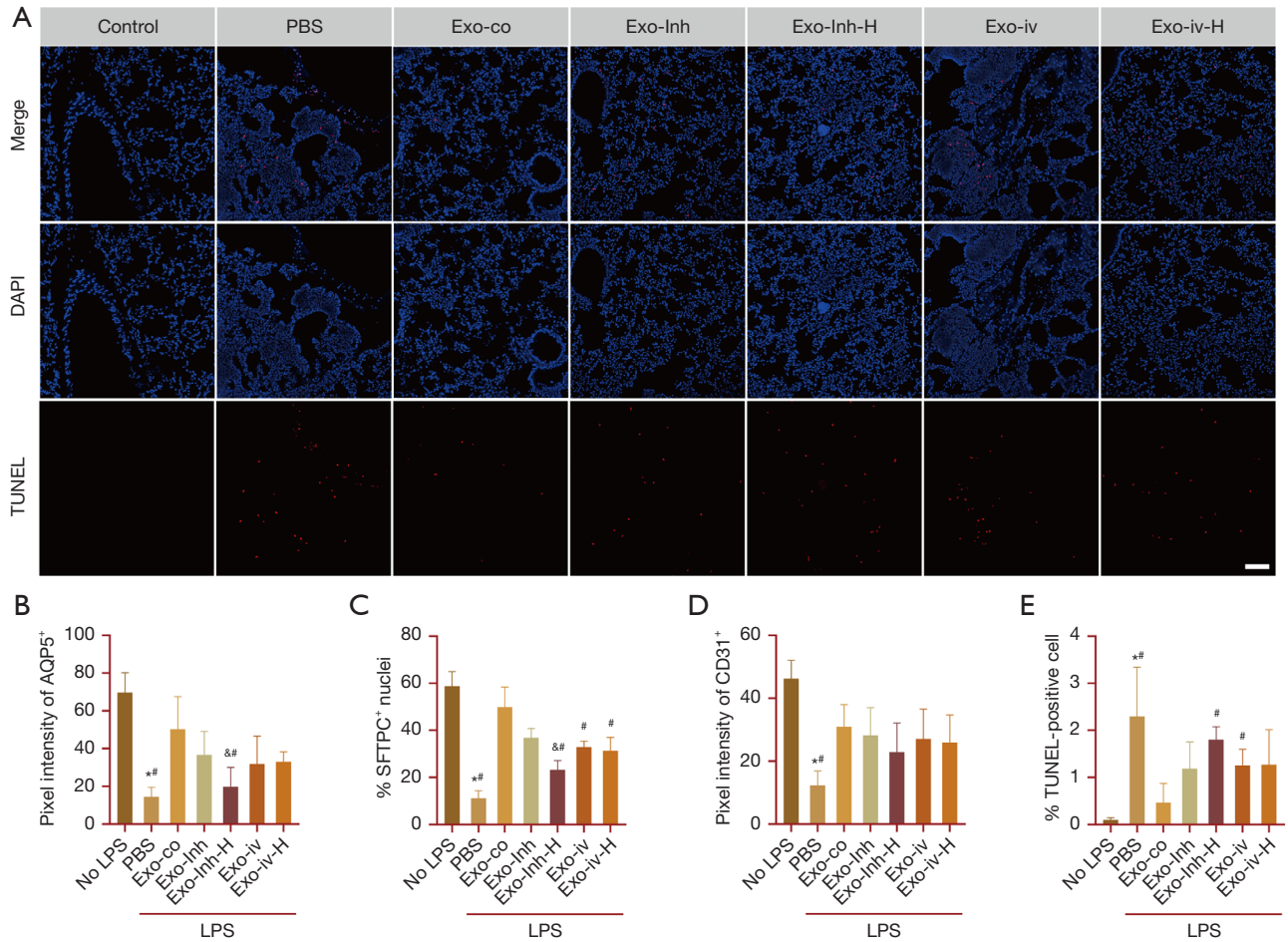

Figure 6 MSC-exo dual channel therapy reduces apoptosis in lung cells. (A) TUNEL staining of apoptotic cells for each group. Scale bar =50 μm. (B-E) Quantification of percent pixel intensity: (B) AQP5$^+$, (C) SFTPC+, (D) CD31$^+$, and (E) TUNEL. Each animal was assessed using three visual fields. N=5 animals. Scores was averaged from one blinded and two non-blinded scorers. *, P<0.05 *vs.* no LPS; $^{\#}$, P<0.05 *vs.* Exo-co; $^{\&}$, P<0.05 *vs.* Exo-Inh. AQP5, aquaporin 5; CD31, platelet endothelial cell adhesion molecule-1; DAPI, 4',6-diamidino-2-phenylindole; Exo-co, exosome dual-route administration; Exo-Inh, exosome nebulization; Exo-Inh-H, high-dose exosome nebulization; Exo-iv, exosome tail vein injection; Exo-iv-H, high-dose exosome tail vein injection; LPS, lipopolysaccharide; MSC-exo, mesenchymal stem cell-derived exosomes; PBS, phosphate-buffered saline; SFTPC, surfactant protein C; TUNEL, Terminal deoxynucleotidyl transferase dUTP Nick End Labeling.

in BALF from ARDS mice suggested significant differences, particularly in the Exo-co group compared to the Exo-Inh-H, Exo-iv, and Exo-iv-H groups (*Figure 7G*,*7H*).

Altered expression of transcriptional programs in ARDS group and Exo-co group

We conducted transcriptome sequencing on mouse lung tissues to explore the differences between the ARDS group and Exo-co group. Next, we performed a differential analysis and identified 671 differentially expressed genes (DEGs) of mouse lung tissues with ARDS group and Exo-co group (*Figure 8A*,*8B*), which included 388 upregulated and 283 downregulated DEGs. These DEGs were mainly enriched during angiogenesis, morphogenesis of an epithelium, mesenchyme development, vascular smooth muscle cell signaling pathways (*Figure 8C*). Additionally, regulation of IL-1 beta production, and regulation of IL-8 biosynthetic process, and inflammasome complex were mainly involved in these DEGs (*Figure 8D*). Furthermore, we performed Gene Set Enrichment Analysis (GSEA) analysis and found statistically significant differences in

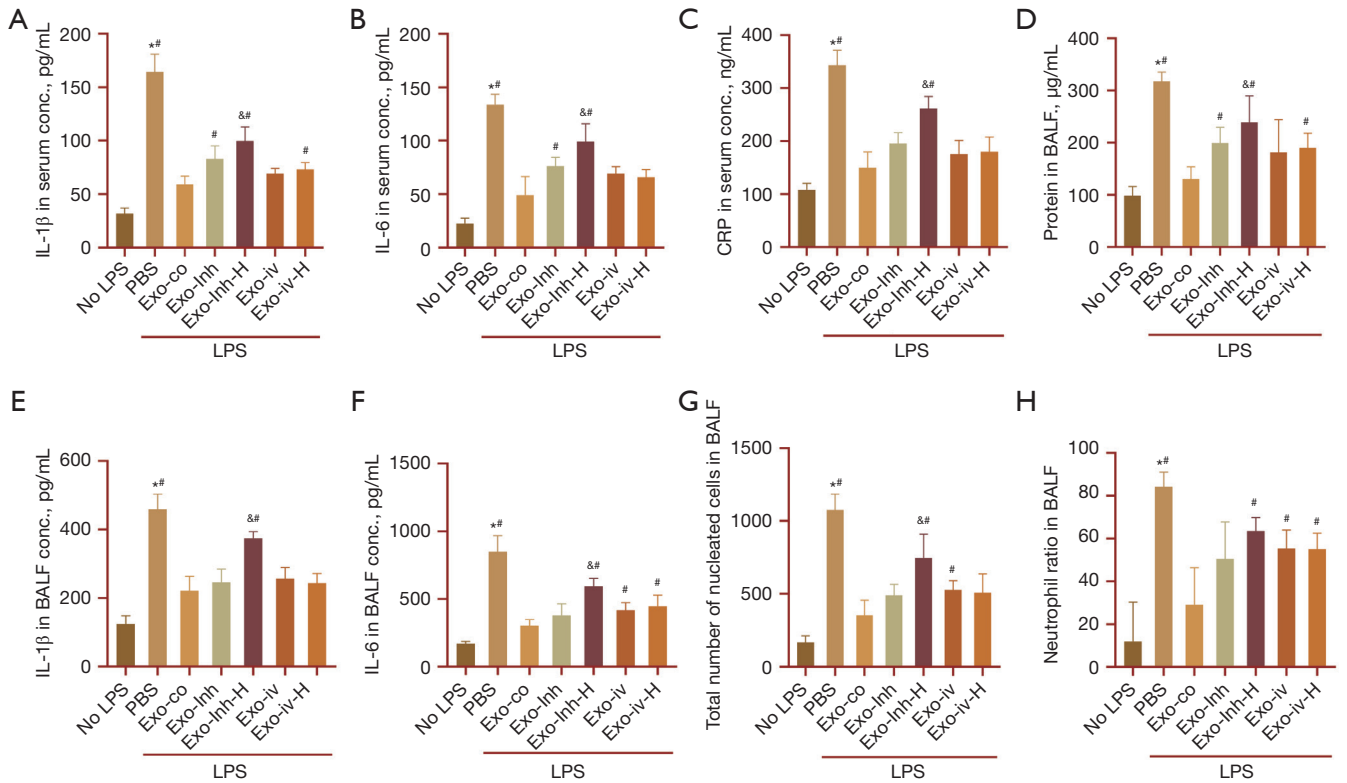

Figure 7 MSC-exo inhibits immune effects induced by LPS in serum and BALF of mice. (A-C) Measurements of the following factors in mouse peripheral serum: IL-1β (A), IL-6 (B), and CRP (C). (D-H) Measurements of the following factors in BALF from mice: protein (D), IL-1β (E), IL-6 (F), total number of nucleated cells (G), and neutrophil ratio (H). N=6 animals. *, P<0.05 *vs.* no LPS; #, P<0.05 *vs.* Exo-co; &, P<0.05 *vs.* Exo-Inh. BALF, bronchoalveolar lavage fluid; conc., concentration; CRP, C-reactive protein; Exo-co, exosome dual-route administration; Exo-Inh, exosome nebulization; Exo-Inh-H, high-dose exosome nebulization; Exo-iv, exosome tail vein injection; Exo-iv-H, high-dose exosome tail vein injection; IL, interleukin; LPS, lipopolysaccharide; MSC-exo, mesenchymal stem cell-derived exosomes; PBS, phosphatebuffered saline.

the pathways of vascular endothelial cell proliferation, regulation of cellular response to transforming growth factor beta stimulus and regulation of endothelial cell differentiation between the two groups (*Figure 8E*).

Discussion

ARDS, as the most common complication and manifestation of COVID-19, has become an important link in the diagnosis and treatment of COVID-19 and has attracted great attention from the scientific community (31). Currently, most animal models replicating known ARDS risk factors *in vivo* are used to simulate the pathological characteristics of human ARDS. However, these models still fail to fully replicate the features of human ARDS. LPS, due to its ease of administration and high reproducibility, is widely employed in ARDS research (16). In this study, to better simulate the characteristics of human ARDS, we selected intratracheal instillation of LPS as our modeling approach. The results showed that LPS-induced ARDS model in mice exhibited distinctive features such as alveolar wall thickening, neutrophil infiltration, and alveolar cavity exudation. These characteristics mirror lung tissue injury hallmarks, suggesting that intratracheal LPS instillation reasonably simulates ARDS and to a certain extent replicates its pathophysiological processes. In 2021, researchers from Shanghai Rui Jin Hospital ascertained through *in vivo* DiR-labeled human adipose-derived mesenchymal stem cell extracellular vesicles (haMSC-EVs) distribution that fluorescence intensity in the lungs reached its peak 24 hours post-nebulization (15). This crucial finding established a pivotal basis for selecting the 24-hour observation time point.

Currently, MSC-exo have been extensively demonstrated to possess potent anti-inflammatory, anti-apoptotic, and

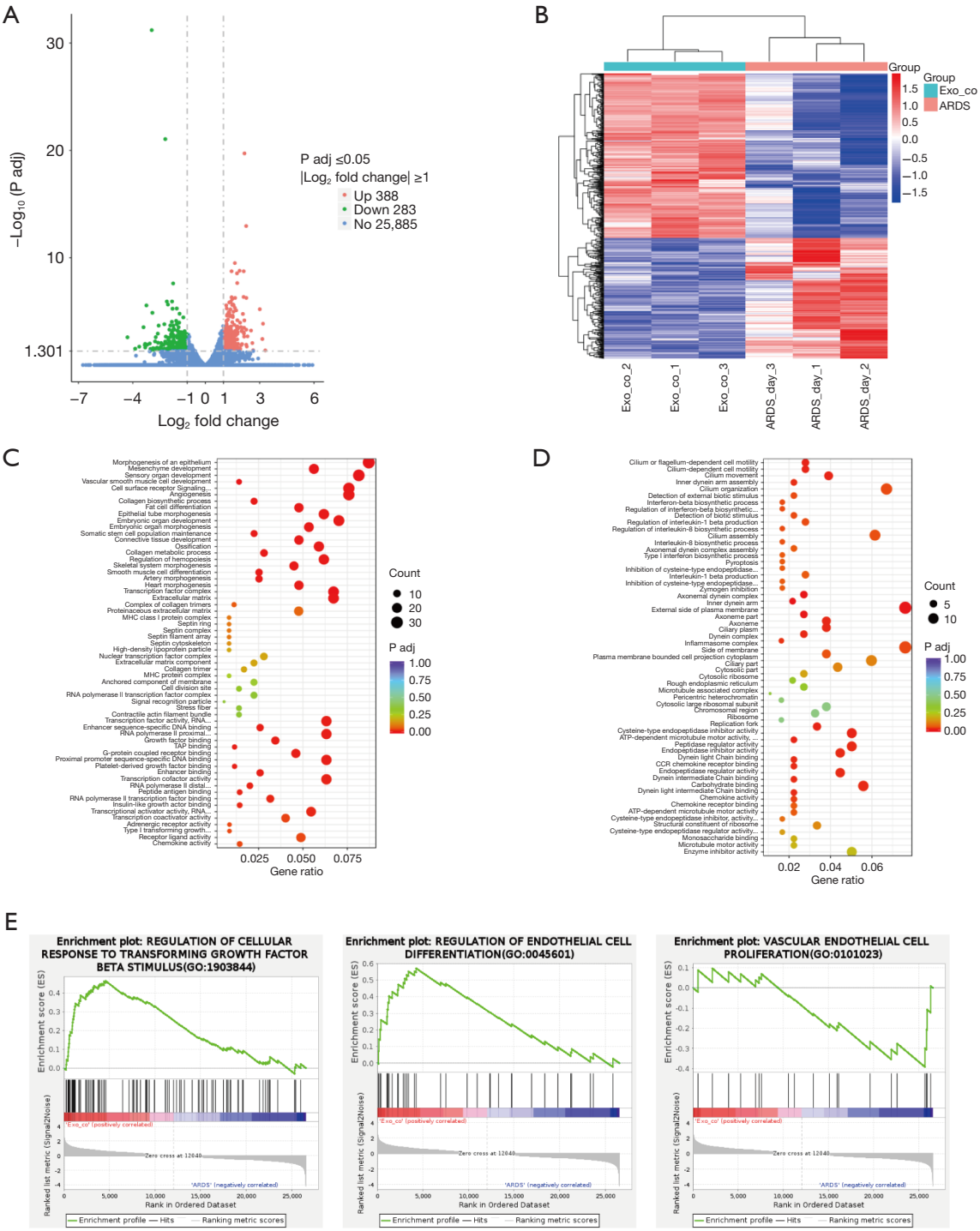

Figure 8 Comparative transcriptome analysis of ARDS group and Exo-co group. (A) Volcano plots showing differentially expressed genes of ARDS group and Exo-co group. Genes with the largest fold change (FC) in differential expression are labeled. (B) Heat map of differentially expressed gene between ARDS group and Exo-co group. (C,D) Biological processes of differentially expressed gene enrichment. The size of the dot corresponds to the gene count. The depth of the color represents the FDR. (E) Gene set enrichment analysis results between ARDS group and Exo-co group. ARDS, acute respiratory distress syndrome; Exo-co, exosome dual-route administration; FDR, false discovery rate.

tissue-repairing functions across various disease models, including pulmonary fibrosis, sepsis, myocardial infarction, and acute kidney injury. Compared to existing standard supportive therapies, the advantage of MSC-exo lies in their ability to target the core pathophysiological processes of ARDS. In contrast to pharmaceutical agents such as corticosteroids, MSC-exo can overcome the limitations of single-target inhibition and avoid the infection risks associated with steroid therapy. Clinically, patients with ARDS usually present with respiratory distress and intractable hypoxemia; their pathophysiologic changes are reduced lung compliance with decreased lung volumes and ventilation (32). Therefore, protective lung ventilation strategies are also commonly used to improve patients' oxygenation and respiratory function in clinical decision-making for the treatment of ARDS (33). At the beginning of the study, we focused our attention on the clinical signs after the intervention in traumatized animals. The results showed that MSC-exo improved oxygen saturation and respiratory function in mice regardless of the concentration or mode of administration, suggesting its effectiveness in the treatment of ARDS. The oxygen saturation level of mice after dual-channel administration was close to normal, suggesting the superiority of dual-channel administration. ARDS has a very high mortality rate in the acute phase, and we collected the 7-day survival of injured mice, and found that MSC-exo was effective in slowing down the mortality rate in the acute phase. Among them, the 7-day survival rate of dual-channel co-administration reached 100%. Similarly, ARDS induced by LPS shares similar pathological lung presentations with COVID-19 patients, both manifesting as diffuse alveolar damage and injury to alveolar epithelial cells and pulmonary microvascular endothelial cells (34). Previous studies have demonstrated that the loss and functional inactivation of AT1 and AT2 cell populations are considered crucial factors contributing to the progression of ARDS (35). In recent years, numerous studies have shown that the severity of ARDS is closely related to the apoptosis of AT1 and AT2 cell populations. In various mouse experiments, an increase in the apoptosis and autophagy of lung epithelial cells can be observed in ARDS mouse injury models induced by LPS or cecal ligation (35,36). The pulmonary microvascular endothelium is a natural barrier that prevents pathogens and inflammatory cytokines from permeating into the blood (37). LPS damages vascular endothelial cells, thereby disrupting this barrier and leading to endothelial dysfunction, allowing a large number of pro-inflammatory and inflammatory cytokines to enter the alveolar space, exacerbating the inflammatory response (25,38). Therefore, inhibiting the apoptosis of pulmonary epithelial and endothelial cells is an important strategy to reduce pulmonary inflammation. Our RNA-seq data corroborates this conclusion. Our series of studies found that MSC-exo treatment can slow down lung tissue damage. Moreover, dual-route administration of MSC-exo treatment can even restore the damaged lungs to a level similar to the healthy control group. This is manifested by the reduction of lung injury scores, a decrease in the number of apoptotic cells, and a significant reduction in the loss of AT1, AT2, and vascular endothelial cell populations. Looking further, the main pathophysiological mechanism of ARDS is the severe systemic and pulmonary inflammatory response leading to apoptosis and necrosis of a large number of lung capillary endothelial cells and alveolar epithelial cells after injury, pathological increase in alveolar capillary and alveolar epithelial permeability, damage to the air-blood barrier and lung water clearance function, followed by intractable hypoxemia and diffuse pulmonary edema (39). Therefore, we further explored the effects of exosome therapy given in different ways on pulmonary and systemic inflammation and lung tissue cell damage. Typically, elevated cytokines are seen in both COVID-19 patients and ARDS patients, especially IL-6, IL-1β, and TNF-α (40,41). Some studies have also focused on the reduction of lymphocytes and high levels of CRP in COVID-19 patients (42,43). In this study, we observed that at the 24-hour time point, whether it was indicators reflecting systemic inflammatory conditions like CRP, or inflammatory indicators in BALF, dual-channel co-administration minimizes inflammatory factor levels.

In addition to discovering the huge advantages of dual channel drug delivery, we have also discovered some interesting things. We found the treatment level reached by the Exo-Inh group and the Exo-iv group was close. However, the dose used by the Exo-Inh group (0.002×10^9 vesicles) was only 1/500 of the Exo-iv group (1×10^9 vesicles). This indicates that with fewer MSC-exo, simple exosome nebulization administration can reach lung tissue more directly, reduce capillary leakage, alleviate alveolar epithelial cell damage, and reduce lung inflammation. Interestingly, we found that when the nebulization administration dose was increased to the same dose as the combined administration (equivalent to a 500-fold increase), the control effect on inflammation was reduced. This is consistent with the results of the team from the Department of Critical Care Medicine at Ruijin Hospital, indicating that there is an appropriate dose for exosome nebulization treatment (15).

Considering that the deposition of aerosols in the lungs is influenced by various factors including the particle size of the inhaled aerosol, inhalation flow rate, inhalation method, and the type, we analyze that taking an excessively large dose of exosome nebulization may block the terminal airways that are already inflamed and narrowed or collapsed, resulting in a decrease in the actual number of exosomes entering the alveoli, and thus a better therapeutic effect cannot be achieved (44). Notably, Qu's team conducted in-depth research on exosome dosage and administration routes, demonstrating that intravenous delivery exhibited superior therapeutic efficacy compared to intranasal and nebulization approaches at specific test dosages. Although some indicators did not show a dose-dependent response to drug concentration, no reduction in therapeutic effect was observed at higher exosome doses. We speculate that this may be attributed to differences in our administration frequency and timing. Their team administered exosomes at 4 and 24 hours, respectively, which effectively leveraged the protective and reparative functions of exosomes. We plan to further investigate this aspect in future studies (45). Moreover, a 2020 study found that the efficiency of nebulization is also affected by the IT to total respiratory cycle time ratio, and patients with ARDS have severe symptoms, especially noticeable respiratory symptoms (46). Therefore, their nebulization efficiency would be greatly affected, and relying solely on nebulized inhalation may not achieve the best therapeutic effect for ARDS. Multiple clinical trials have shown that intravenous infusion of MSCs is effective and safe for COVID-19 patients, especially for moderate to severe patients (47-49). In this study, the advantage of Exo-iv group was not obvious after 24 hours of administration; however, after 72 hours of administration, we monitored the blood oxygen saturation of mice and found that Exo-iv and Exo-iv-H groups were significantly better than Exo-Inh group. Analyzing the reasons for the above phenomena, we believe that it is due to the fact that MSC-exo intravenous administration reaches various organs through the systemic blood circulation, and it has a stronger effect in controlling the systemic inflammatory response. Therefore, through the systemic blood circulation system, it will delay its arrival at various organs and the lungs, and the damaged endothelial cells will quickly absorb MSC-exo after intravenous injection. There will be a certain degree of MSC-exo loss for a short time after intravenous administration, which reduces the number reaching distant target organ sites. Based on the above analysis, we believe that because the time for intravenous infusion to take effect is slightly longer than nebulization, nebulization inhalation treatment can be an important supplementary treatment.

However, in this study, MSC-exo showed less than expected efficacy in improving vascular endothelial cell (CD31) function and blood vessel permeability index (BCA). Our analysis revealed no significant differences between the Exo-co group and other control groups in these metrics. This discrepancy may stem from asynchronous mechanisms: while exosomes administered via tail vein infusion could delay systemic inflammatory response suppression and vascular endothelial damage resolution through circulation, we failed to validate pulmonary function, tissue injury, or cytokine levels at 72-hour and 7-day time points. Consequently, our 24-hour observation window was insufficient to capture these delayed effects. Also, in this study, we were not able to explore the best dosage for intravenous administration. Our future research will further extend the observation time and explore the therapeutic differences brought about by different intravenous administration doses. Currently, we are trying to establish a mouse ARDS model with tail vein and intraperitoneal injection of LPS to further explore the different therapeutic outcomes brought about by different modeling methods.

Conclusions

In summary, we demonstrated that dual-route administration of MSC-exo through nebulization and tail vein, not only controls the systemic inflammation of ARDS, but also addresses the local lung injury, exhibited a beneficial effect in LPS-ARDS in mice. Combining the characteristics of ARDS disease itself, we recommend different treatment plans for different patients. For whom with severe systemic and respiratory system inflammation, dual-route combination therapy could improve the prognosis of patients by controlling their systemic inflammation and improving their respiratory function at the same time, and or whom with mild illness but obvious respiratory symptoms, small-dose nebulization treatment may suffice (*Figure 9*). Therefore, this could be a novel and potential mode for cell-free treatment of ARDS.

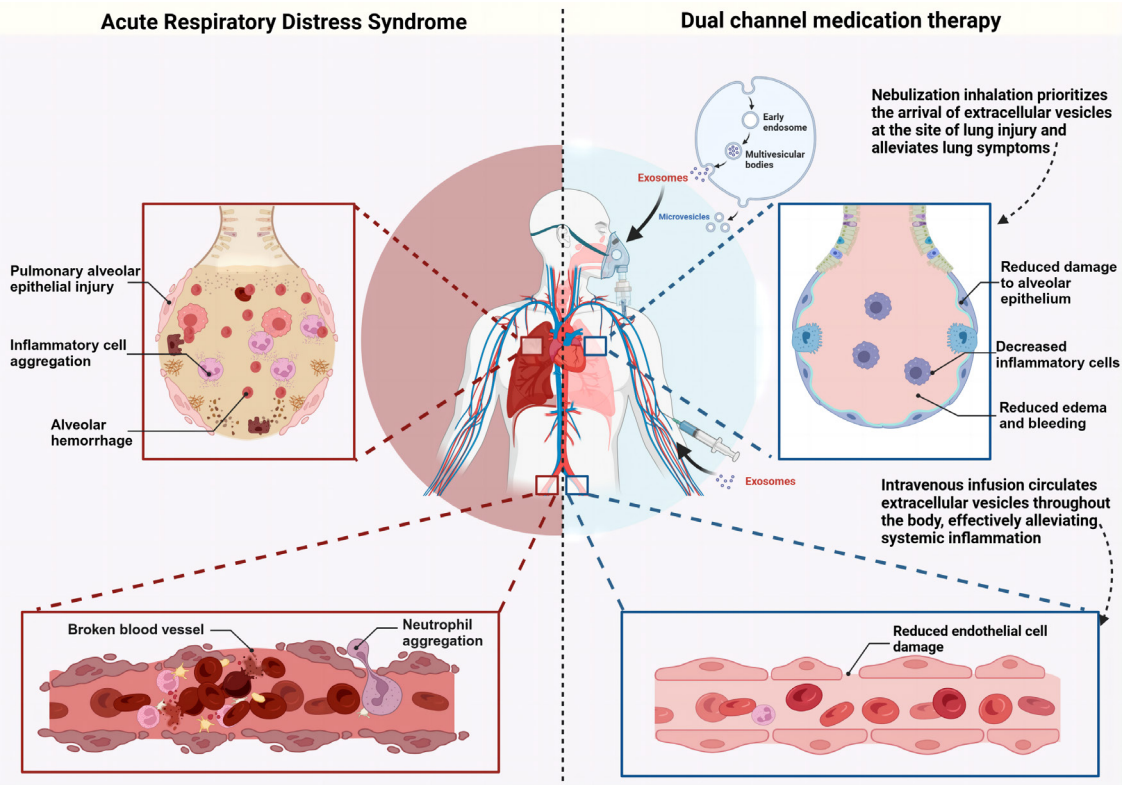

Figure 9 Schematic diagram of dual channel combined administration method.

Acknowledgments

We are grateful to Beijing Tuberculosis and Thoracic Tumor Research Institute for providing the experimental platform and support, as well as the teachers of the Department of Respiratory Medicine, Cancer Research Center and Department of Pathology for their great support.

Footnote

Reporting Checklist: The authors have completed the ARRIVE reporting checklist. Available at https://jtd.amegroups.com/article/view/10.21037/jtd-2025-250/rc

Data Sharing Statement: Available at https://jtd.amegroups.com/article/view/10.21037/jtd-2025-250/dss

Peer Review File: Available at https://jtd.amegroups.com/article/view/10.21037/jtd-2025-250/prf

Funding: This study was supported by the National Natural Science Foundation of China (grant No. 82273130), Beijing Municipal Natural Science Foundation (grant No. L234007), The Cultivation Project of Beijing Municipal Hospital Administration (PX2023059), and Beijing CSCO Clinical Oncology Research Foundation (grant No. Y-HR2020MS-0156).

Conflicts of Interest: All authors have completed the ICMJE uniform disclosure form (available at https://jtd.amegroups.com/article/view/10.21037/jtd-2025-250/coif). The authors have no conflicts of interest to declare.

Ethical Statement: The authors are accountable for all aspects of the work in ensuring that questions related to the accuracy or integrity of any part of the work are appropriately investigated and resolved. The experiments were performed under a project license (No. xk2022-080) granted by the Animal Experiment Ethics Committee of Beijing Chest Hospital, Capital Medical University, in compliance with the institutional guidelines for the care and use of animals.

Open Access Statement: This is an Open Access article

References

1. Meyer NJ, Gattinoni L, Calfee CS. Acute respiratory distress syndrome. Lancet 2021;398:622-37.
2. Hasan SS, Capstick T, Ahmed R, et al. Mortality in COVID-19 patients with acute respiratory distress syndrome and corticosteroids use: a systematic review and meta-analysis. Expert Rev Respir Med 2020;14:1149-63.
3. Yang X, Yu Y, Xu J, et al. Clinical course and outcomes of critically ill patients with SARS-CoV-2 pneumonia in Wuhan, China: a single-centered, retrospective, observational study. Lancet Respir Med 2020;8:475-81.
4. Chung KP, Cheng CN, Chen YJ, et al. Alveolar epithelial cells mitigate neutrophilic inflammation in lung injury through regulating mitochondrial fatty acid oxidation. Nat Commun 2024;15:7241.
5. Huppert LA, Matthay MA, Ware LB. Pathogenesis of Acute Respiratory Distress Syndrome. Semin Respir Crit Care Med 2019;40:31-9.
6. Bernard GR, Artigas A, Brigham KL, et al. The American-European Consensus Conference on ARDS. Definitions, mechanisms, relevant outcomes, and clinical trial coordination. Am J Respir Crit Care Med 1994;149:818-24.
7. National Heart, Lung, and Blood Institute Acute Respiratory Distress Syndrome (ARDS) Clinical Trials Network; Wiedemann HP, Wheeler AP, et al. Comparison of two fluid-management strategies in acute lung injury. N Engl J Med 2006;354:2564-75.
8. Yáñez-Mó M, Siljander PR, Andreu Z, et al. Biological properties of extracellular vesicles and their physiological functions. J Extracell Vesicles 2015;4:27066.
9. Dauletova M, Hafsan H, Mahhengam N, et al. Mesenchymal stem cell alongside exosomes as a novel cell-based therapy for COVID-19: A review study. Clin Immunol 2021;226:108712.
10. Kaspi H, Semo J, Abramov N, et al. MSC-NTF (NurOwn®) exosomes: a novel therapeutic modality in the mouse LPS-induced ARDS model. Stem Cell Res Ther 2021;12:72.
11. Li X, Wang S, Zhu R, et al. Lung tumor exosomes induce a pro-inflammatory phenotype in mesenchymal stem cells via NFκB-TLR signaling pathway. J Hematol Oncol 2016;9:42.
12. Dinh PC, Paudel D, Brochu H, et al. Inhalation of lung spheroid cell secretome and exosomes promotes lung repair in pulmonary fibrosis. Nat Commun 2020;11:1064.
13. Shah TG, Predescu D, Predescu S. Mesenchymal stem cells-derived extracellular vesicles in acute respiratory distress syndrome: a review of current literature and potential future treatment options. Clin Transl Med 2019;8:25.
14. Meng F, Xu R, Wang S, et al. Human umbilical cord-derived mesenchymal stem cell therapy in patients with COVID-19: a phase 1 clinical trial. Signal Transduct Target Ther 2020;5:172.
15. Shi MM, Yang QY, Monsel A, et al. Preclinical efficacy and clinical safety of clinical-grade nebulized allogenic adipose mesenchymal stromal cells-derived extracellular vesicles. J Extracell Vesicles 2021;10:e12134.
16. Matute-Bello G, Frevert CW, Martin TR. Animal models of acute lung injury. Am J Physiol Lung Cell Mol Physiol 2008;295:L379-99.
17. Li JW, Wei L, Han Z, et al. Mesenchymal stromal cells-derived exosomes alleviate ischemia/reperfusion injury in mouse lung by transporting anti-apoptotic miR-21-5p. Eur J Pharmacol 2019;852:68-76.
18. Matute-Bello G, Downey G, Moore BB, et al. An official American Thoracic Society workshop report: features and measurements of experimental acute lung injury in animals. Am J Respir Cell Mol Biol 2011;44:725-38.
19. Chen J, Chen J, Cheng Y, et al. Mesenchymal stem cell-derived exosomes protect beta cells against hypoxia-induced apoptosis via miR-21 by alleviating ER stress and inhibiting p38 MAPK phosphorylation. Stem Cell Res Ther 2020;11:97.
20. Kalluri R, LeBleu VS. The biology, function, and biomedical applications of exosomes. Science 2020;367:eaau6977.
21. Yu M, Liu W, Li J, et al. Exosomes derived from atorvastatin-pretreated MSC accelerate diabetic wound repair by enhancing angiogenesis via AKT/eNOS pathway. Stem Cell Res Ther 2020;11:350.
22. Yang L, Zhou F, Zheng D, et al. FGF/FGFR signaling: From lung development to respiratory diseases. Cytokine Growth Factor Rev 2021;62:94-104.
23. Shiraishi K, Shah PP, Morley MP, et al. Biophysical forces mediated by respiration maintain lung alveolar epithelial

cell fate. Cell 2023;186:1478-1492.e15.
24. Desai TJ, Brownfield DG, Krasnow MA. Alveolar progenitor and stem cells in lung development, renewal and cancer. Nature 2014;507:190-4.
25. Maniatis NA, Kotanidou A, Catravas JD, et al. Endothelial pathomechanisms in acute lung injury. Vascul Pharmacol 2008;49:119-33.
26. Liu L, Shi GP. CD31: beyond a marker for endothelial cells. Cardiovasc Res 2012;94:3-5.
27. Villar J, Zhang H, Slutsky AS. Lung Repair and Regeneration in ARDS: Role of PECAM1 and Wnt Signaling. Chest 2019;155:587-94.
28. Sauler M, Bazan IS, Lee PJ. Cell Death in the Lung: The Apoptosis-Necroptosis Axis. Annu Rev Physiol 2019;81:375-402.
29. Amulic B, Cazalet C, Hayes GL, et al. Neutrophil function: from mechanisms to disease. Annu Rev Immunol 2012;30:459-89.
30. Boechat JL, Chora I, Morais A, et al. The immune response to SARS-CoV-2 and COVID-19 immunopathology -- Current perspectives. Pulmonology 2021;27:423-37.
31. Asselah T, Durantel D, Pasmant E, et al. COVID-19: Discovery, diagnostics and drug development. J Hepatol 2021;74:168-84.
32. ARDS Definition Task Force, Ranieri VM, Rubenfeld GD, et al. Acute respiratory distress syndrome: the Berlin Definition. JAMA 2012;307:2526-33.
33. Acute Respiratory Distress Syndrome Network, Brower RG, Matthay MA, et al. Ventilation with lower tidal volumes as compared with traditional tidal volumes for acute lung injury and the acute respiratory distress syndrome. N Engl J Med 2000;342:1301-8.
34. Qiao Q, Liu X, Yang T, et al. Nanomedicine for acute respiratory distress syndrome: The latest application, targeting strategy, and rational design. Acta Pharm Sin B 2021;11:3060-91.
35. Cui H, Xie N, Banerjee S, et al. Impairment of Fatty Acid Oxidation in Alveolar Epithelial Cells Mediates Acute Lung Injury. Am J Respir Cell Mol Biol 2019;60:167-78.
36. Wu J, Wang Y, Liu G, et al. Characterization of air-liquid interface culture of A549 alveolar epithelial cells. Braz J Med Biol Res 2017;51:e6950.
37. Li L, Wei J, Mallampalli RK, et al. TRIM21 Mitigates Human Lung Microvascular Endothelial Cells' Inflammatory Responses to LPS. Am J Respir Cell Mol Biol 2019;61:776-85.
38. Stevens T. Functional and molecular heterogeneity of pulmonary endothelial cells. Proc Am Thorac Soc 2011;8:453-7.
39. Bos LDJ, Ware LB. Acute respiratory distress syndrome: causes, pathophysiology, and phenotypes. Lancet 2022;400:1145-56.
40. Ramasamy S, Subbian S. Critical Determinants of Cytokine Storm and Type I Interferon Response in COVID-19 Pathogenesis. Clin Microbiol Rev 2021;34:e00299-20.
41. Chen G, Wu D, Guo W, et al. Clinical and immunological features of severe and moderate coronavirus disease 2019. J Clin Invest 2020;130:2620-9.
42. Wang D, Hu B, Hu C, et al. Clinical Characteristics of 138 Hospitalized Patients With 2019 Novel Coronavirus-Infected Pneumonia in Wuhan, China. JAMA 2020;323:1061-9.
43. Chen N, Zhou M, Dong X, et al. Epidemiological and clinical characteristics of 99 cases of 2019 novel coronavirus pneumonia in Wuhan, China: a descriptive study. Lancet 2020;395:507-13.
44. Schwarz C, Procaccianti C, Costa L, et al. Differential Performance and Lung Deposition of Levofloxacin with Different Nebulisers Used in Cystic Fibrosis. Int J Mol Sci 2022;23:9597.
45. Chen J, Liu S, Zou J, et al. Comparison of efficacy of exosomes derived from human umbilical cord blood mesenchymal stem cells in treating mouse acute lung injury via different routes. Front Pediatr 2025;13:1560915.
46. Blais CM, Davis BE, Graham BL, et al. Respiratory Duty Cycles in Individuals With and Without Airway Hyperresponsiveness. Chest 2020;157:356-62.
47. Tang L, Jiang Y, Zhu M, et al. Clinical study using mesenchymal stem cells for the treatment of patients with severe COVID-19. Front Med 2020;14:664-73.
48. Shi L, Wang L, Xu R, et al. Mesenchymal stem cell therapy for severe COVID-19. Signal Transduct Target Ther 2021;6:339.
49. Leng Z, Zhu R, Hou W, et al. Transplantation of ACE2(-) Mesenchymal Stem Cells Improves the Outcome of Patients with COVID-19 Pneumonia. Aging Dis 2020;11:216-28.

Cite this article as: Yang L, Cao Z, Xing Y, Pan Y, Yang C, Zhang L, Zhao H, Ma T, Ye H. Inhalation & intravenous: umbilical cord mesenchymal stem cell-derived exosomes therapy strategy for acute respiratory distress syndrome in a murine model. J Thorac Dis 2025;17(12):11100-11117. doi: 10.21037/jtd-2025-250

